Kondo Breakdown in a Spin-1/2 Chain of Adatoms on a Dirac Semimetal

Bimla Danu,[1,*] Matthias Vojta,[2,†] Fakher F. Assaad,[1,‡] and Tarun Grover[3,§]
[1]*Institut für Theoretische Physik und Astrophysik and Würzburg-Dresden Cluster of Excellence ct.qmat, Universität Würzburg, 97074 Würzburg, Germany*
[2]*Institut für Theoretische Physik and Würzburg-Dresden Cluster of Excellence ct.qmat, Technische Universität Dresden, 01062 Dresden, Germany*
[3]*Department of Physics, University of California at San Diego, La Jolla, California 92093, USA*

(Received 8 June 2020; accepted 2 October 2020; published 13 November 2020)

We consider a spin-1/2 Heisenberg chain coupled via a Kondo interaction to two-dimensional Dirac fermions. The Kondo interaction is irrelevant at the *decoupled* fixed point, leading to the existence of a Kondo-breakdown phase and a Kondo-breakdown critical point separating such a phase from a heavy Fermi liquid. We reach this conclusion on the basis of a renormalization group analysis, large-N calculations as well as extensive auxiliary-field quantum Monte Carlo simulations. We extract quantities such as the zero-bias tunneling conductance which will be relevant to future experiments involving adatoms on semimetals such as graphene.

DOI: 10.1103/PhysRevLett.125.206602

The antiferromagnetic Kondo coupling J_k between a spin-1/2 degree of freedom and a Fermi sea with finite density of states at the Fermi energy is (marginally) relevant: J_k flows to strong coupling and the impurity is screened. If, in contrast, the density of states shows a power-law pseudogap behavior, the Kondo coupling is irrelevant at the decoupled fixed point, and the spin remains unscreened at weak coupling. Since for strong Kondo coupling screening is present, a nontrivial Kondo-breakdown quantum critical point emerges [1–3]. The decoupled and the Kondo-screened phases share the same symmetry properties.

In the context of Kondo lattices, the numbers of both conduction electrons and impurity spins scale with the volume of the system. In the Kondo-screened paramagnetic (i.e., heavy Fermi-liquid) phase, the volume enclosed by the Fermi surface (i.e., Luttinger volume) counts both spins and electrons. A Kondo-breakdown transition (equivalently, an orbital-selective Mott transition [4]), which, as above, does not involve symmetry breaking, implies that the spins drop out from the Luttinger count. For the case of an odd number of electrons and spins per unit cell, this leads to a violation of the Luttinger sum rule. Oshikawa's flux-threading argument [5,6] shows that a specific family of the resulting states of matter can be achieved via topological degeneracy in the spin sector [7]. Such states, coined fractionalized Fermi liquid (FL*) phases, have been realized numerically [8]. Kondo breakdown has also been proposed to understand the phenomenology of heavy-fermion systems [7,9,10], especially in the context of materials such as $YbRh_2Si_2$ and $CeCu_{6-x}Au_x$ [11,12].

In this Letter, we consider a situation intermediate between Kondo impurity and Kondo lattice: a one-dimensional (1D) Heisenberg chain which is Kondo coupled to two-dimensional Dirac electrons. Dimensional analysis shows that, at the decoupled fixed point, the Kondo coupling is irrelevant, thus leading to an RG flow very similar to that of the pseudogap Kondo effect discussed above, see Fig. 1. The motivation to study such systems equally stems from scanning tunneling microscopy (STM) experiments of Co adatoms on a $Cu_2N/Cu(100)$ surface. Here, recent experiments show an impressive ability to tune the exchange coupling between adatoms as well as the coupling of adatoms to the surface [13–19]. As shown in Ref. [20], simple models amenable to negative-sign-free quantum Monte Carlo (QMC) simulations are able to provide a detailed account of the experiments. Another experimental system that has qualitative resemblance with our setup is Yb_2Pt_2Pb, where neutron scattering indicates the presence of 1D spinons, and an apparent absence of Kondo screening, despite the presence of three-dimensional conduction electrons [21–23]. In our study, we consider conduction electrons in two dimensions with Dirac spectrum since this choice unambiguously leads to a Kondo-breakdown phase and phase transition, while also allowing RG and large-N calculations and explicit comparison to QMC numerics.

Model Hamiltonian.—We consider a spin-1/2 Heisenberg chain on a semimetallic substrate:

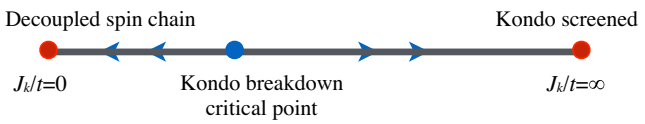

FIG. 1. Renormalization group flow of the Kondo coupling J_k for a spin-1/2 chain on a semimetallic substrate.

$$\hat{H} = -t\sum_{\langle \boldsymbol{i},\boldsymbol{j}\rangle}(e^{2\pi i/\Phi_0\int_i^j \boldsymbol{A}\cdot d\boldsymbol{l}}\hat{\boldsymbol{c}}_{\boldsymbol{i}}^{\dagger}\hat{\boldsymbol{c}}_{\boldsymbol{j}} + \text{H.c.}) + \frac{J_k}{2}\sum_{l=1}^{L}\hat{\boldsymbol{c}}_{\boldsymbol{l}}^{\dagger}\boldsymbol{\sigma}\hat{\boldsymbol{c}}_{\boldsymbol{l}}\cdot\hat{\boldsymbol{S}}_{\boldsymbol{l}} + J_h\sum_{l=1}^{L}\hat{\boldsymbol{S}}_{\boldsymbol{l}}\cdot\hat{\boldsymbol{S}}_{\boldsymbol{l}+\Delta\boldsymbol{l}}. \quad (1)$$

Here, t is the hopping parameter of the conduction electrons, the summation $\sum_{\langle \boldsymbol{i},\boldsymbol{j}\rangle}$ runs over a square lattice and $\hat{\boldsymbol{c}}_{\boldsymbol{i}}^{\dagger} = (\hat{c}_{\boldsymbol{i},\uparrow}^{\dagger}, \hat{c}_{\boldsymbol{i},\downarrow}^{\dagger})$ is a spinor where $\hat{c}_{\boldsymbol{i},\uparrow(\downarrow)}^{\dagger}$ creates an electron at site $\boldsymbol{i}$ with z component of spin $1/2$ $(-1/2)$. We use the Landau gauge, $\boldsymbol{A} = B(-y, 0, 0)$, and tune B such that half a flux quantum (π flux) pierces each plaquette. This gauge choice allows for translation symmetry by one lattice site in the x direction. $J_k > 0$ is the antiferromagnetic Kondo coupling between magnetic adatoms and conduction electrons, $J_h > 0$ the Heisenberg coupling between magnetic adatoms, L the length of the Heisenberg chain and linear length of the square conduction electron lattice, and $\hat{\boldsymbol{S}}_{\boldsymbol{l}}$ represents the spin-$1/2$ operators. We use an array of adatoms at interatomic distance $\Delta\boldsymbol{l} = (a, 0)$ on the substrate and choose periodic boundary conditions. Hereafter, we set $a = 1$.

RG analysis.—Consider the Hamiltonian in Eq. (1) at $J_k = 0$. At low energies, this describes two decoupled theories, both of which are scale invariant: the fermions are described by the massless $(2+1)$-dimensional free Dirac Hamiltonian, while the spin-$1/2$ Heisenberg chain is described by a Luttinger liquid [24]. In a $(d+1)$-dimensional free Dirac theory, the correlation functions of operator $\hat{\boldsymbol{c}}^{\dagger}\boldsymbol{\sigma}\hat{\boldsymbol{c}}$ decay as $\langle\hat{\boldsymbol{c}}^{\dagger}(x)\boldsymbol{\sigma}\hat{\boldsymbol{c}}(x)\hat{\boldsymbol{c}}^{\dagger}(0)\boldsymbol{\sigma}\hat{\boldsymbol{c}}(0)\rangle \sim 1/x^{2d}$, therefore, the scaling dimension of this operator $\Delta_{\hat{\boldsymbol{c}}^{\dagger}\boldsymbol{\sigma}\hat{\boldsymbol{c}}} = d$ [25]. Similarly, for the Heisenberg chain, $\langle\hat{S}(x)\hat{S}(0)\rangle \sim 1/x$ and therefore $\Delta_{\hat{S}} = \frac{1}{2}$. This implies that at this decoupled fixed point, in our case ($d = 2$), the Kondo coupling has a scaling dimension $2 - \Delta_{\hat{\boldsymbol{c}}^{\dagger}\boldsymbol{\sigma}\hat{\boldsymbol{c}}} - \Delta_{\hat{S}} = 2 - d - \frac{1}{2} = -\frac{1}{2}$ and is thereby irrelevant. Therefore, the small-J_k phase is an instance of FL* [7]: a non-symmetry-breaking phase in which two coexisting subsystems—a band of conduction electrons and a fractionalized local-moment spin liquid—are asymptotically decoupled.

On the other hand, in the limit $J_k \to \infty$ each spin-$1/2$ degree of freedom binds in a singlet with a conduction electron. This one-dimensional singlet product state, corresponding to the strong-coupling limit of the one-dimensional Kondo lattice model [26], decouples from the conduction electrons, and effectively changes the boundary condition in the y direction from periodic to open. At large but finite J_k, we expect the system to be locally described by a heavy Fermi liquid. Assuming these two regimes are separated by a single phase transition motivates us to find a suitable RG description of this transition. The approach we follow is to consider $(d+1)$-dimensional Dirac fermions coupled to a $(1+1)$-dimensional Heisenberg chain. By the aforementioned power counting, the Kondo coupling is marginal in $d = 3/2$, which allows for an expansion in $\epsilon = d - 3/2$, where the physical case of interest corresponds to $d = 2$, i.e., $\epsilon = 1/2$. Perturbing around the $J_k = 0$ fixed point, the RG flow of dimensionless Kondo coupling $j_k = J_k\Lambda^{\epsilon}$ is given by

$$\frac{dj_k}{d\ln\Lambda} = \epsilon j_k - \frac{j_k^2}{2}, \quad (2)$$

where Λ is an ultraviolet cutoff, and we have kept terms to $O(j_k^2)$ (see Sec. I of Ref. [27] for details). The resulting flow diagram is shown in Fig. 1 and the Kondo-breakdown critical fixed point is given by $j_k^c = 2\epsilon$, which yields the correlation-length exponent $\nu = 1/\epsilon$. Because of Lorentz invariance, the critical theory will exhibit ω/T scaling in all observables.

Large-N approximation.—To formulate the large-N approximation, we use a fermion representation of the spin degree of freedom, $\hat{\boldsymbol{S}}_{\boldsymbol{l}} = \frac{1}{2}\hat{\boldsymbol{d}}_{\boldsymbol{l}}^{\dagger}\boldsymbol{\sigma}\hat{\boldsymbol{d}}_{\boldsymbol{l}}$ and impose the constraint $\hat{\boldsymbol{d}}_{\boldsymbol{l}}^{\dagger}\hat{\boldsymbol{d}}_{\boldsymbol{l}} = 1$ with $\hat{\boldsymbol{d}}_{\boldsymbol{l}}^{\dagger} = (\hat{d}_{\boldsymbol{l},\uparrow}^{\dagger}, \hat{d}_{\boldsymbol{l},\downarrow}^{\dagger})$. The interaction part of the Hamiltonian can then be written as $-(J_k/4)\sum_{\boldsymbol{l}}(\hat{\boldsymbol{c}}_{\boldsymbol{l}}^{\dagger}\hat{\boldsymbol{d}}_{\boldsymbol{l}} + \text{H.c.})^2 - (J_h/4)\sum_{\boldsymbol{l}}(\hat{\boldsymbol{d}}_{\boldsymbol{l}}^{\dagger}\hat{\boldsymbol{d}}_{\boldsymbol{l}+\Delta\boldsymbol{l}} + \text{H.c.})^2 + (U/2)\sum_{\boldsymbol{l}}(\hat{\boldsymbol{d}}_{\boldsymbol{l}}^{\dagger}\hat{\boldsymbol{d}}_{\boldsymbol{l}} - 1)^2$. Formally, the Hubbard U should be set to infinity so as to enforce no double occupancy on the d electrons; practically, choosing a large enough value of βU ($\gtrsim 10$) suffices. The mean-field variables, $V = \langle\hat{\boldsymbol{c}}_{\boldsymbol{l}}^{\dagger}\hat{\boldsymbol{d}}_{\boldsymbol{l}}\rangle, \chi = \langle\hat{\boldsymbol{d}}_{\boldsymbol{l}}^{\dagger}\hat{\boldsymbol{d}}_{\boldsymbol{l}+\Delta\boldsymbol{l}}\rangle$, are determined self-consistently under the constraint $\langle\hat{\boldsymbol{d}}_{\boldsymbol{l}}^{\dagger}\hat{\boldsymbol{d}}_{\boldsymbol{l}}\rangle = 1$. Figure 2 shows the mean-field result. The details of the calculations are presented in Secs. II and III of Ref. [27]. Within this approximation, the absence of Kondo screening corresponds to $V = 0$ and $\chi \neq 0$, while Kondo screening implies $V \neq 0$ and $\chi \neq 0$. As is apparent, for each value of J_h the mean-field solution shows a single transition. In the limit $J_h = 0$, the critical value of J_k corresponds to that of the single-impurity pseudogap Kondo problem [29]. Aside from the mean-field order parameters, the transition can be detected by considering the spin-spin correlations along the chain. In the

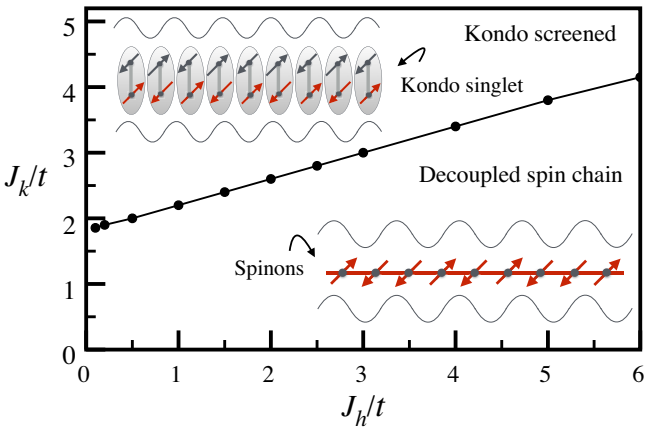

FIG. 2. The zero-temperature mean-field phase diagram in a parameter space of J_k/t and J_h/t.

decoupled phase spinons are confined to the chain and the spin-spin correlations—at the mean-field level—decay as $1/r^2$. In the Kondo-screened phase, spins hybridize with the Dirac electrons. Since the spin system is subextensive, the properties of the Dirac electrons remain unchanged and the spin-spin correlations along the chain inherit the 2D Dirac $1/r^4$ decay (see Fig. S3 of Ref. [27]). Introducing particle-hole asymmetry by adding next-nearest hopping (while keeping a half-filled semimetallic state) was found to lead to similar results within large N [27].

QMC simulations.—We have used the algorithms for lattice fermions (ALF) [31] implementation of the finite-temperature auxiliary-field QMC algorithm [32–37]. The absence of the negative sign problem follows from the standard antiunitary particle-hole transformation [34]. For a given system of linear length L, the QMC simulations are performed at an inverse temperature $\beta t(t/k_B T) = L$ and at a fixed $J_h/t = 1$. At $L = 20$ we checked that the choice $\beta t = 2L$ shows similar results as $\beta t = L$. For the considered periodic boundary conditions, $L = 4n + 2$ corresponds to open-shell configurations and is known to show less finite-size effects than $L = 4n + 4$ sized systems. Finally, we have chosen U large enough so as to guarantee that $\hat{\boldsymbol{d}}_l^\dagger \hat{\boldsymbol{d}}_l = 1$ within our numerical accuracy.

QMC results.—Figure 3 plots the spin-spin correlations $C(r) = 4\langle \hat{S}^z{}_0 \hat{S}^z{}_r \rangle$ as a function of distance r for various values of J_k/t. In the limit of vanishing Kondo coupling, our results are consistent with the exact asymptotic form: $C(r) \propto (-1)^r \sqrt{\ln r}/r$. The $1/r$ decay of the spin-spin correlations in the Heisenberg model is tied to SU(2) spin symmetry. If the Kondo coupling is irrelevant, then we expect the asymptotic form of the spin-spin correlations should continue to follow a $(-1)^r/r$ form. Remarkably, the data support this point of view up to $J_k/t \lesssim 2$. On the other hand, in the Kondo-screened phase for $J_k/t \gtrsim 2$, the equal-time correlations decay with a power larger than unity. In this phase, we expect the spin-spin correlations to inherit the power law of the Dirac fermions $\langle \hat{S}_l^{z,c} \hat{S}_{l+r}^{z,c} \rangle \propto 1/r^4$ (see, Fig. S3 of Ref. [27]). The insets of Fig. 3 plot the static spin structure factor $S(k) = (1/L)\sum_r e^{-ik\cdot r} C(r)$ as a function of momentum k. Noticeably, both at $J_k = 0$ and $J_k/t = 1.5$ we observe systematic growth of $S(k)$ at $k = \pi$, reflecting the $(-1)^r/r$ real-space decay. At $J_k/t = 2$ we observe a cusp feature but a saturation of $S(k = \pi)$ with system size thus suggesting a power law with exponent $1 < K_\sigma < 2$. Finally, in the Kondo-screened phase at $J_k/t = 3$, $S(k)$ converges to a smooth function implying $K_\sigma > 2$. A detailed overview of the QMC data is given in Sec. IV of Ref. [27].

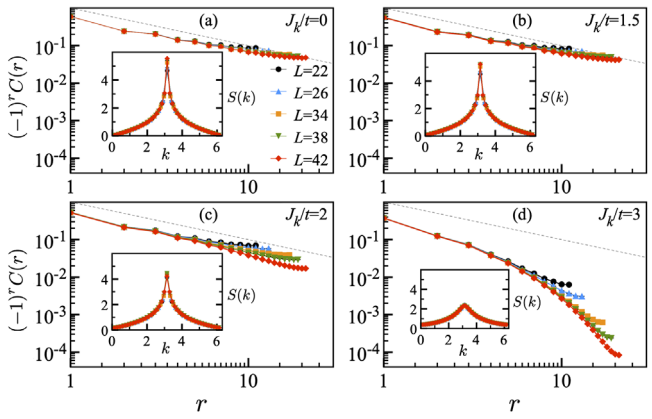

FIG. 3. $C(r)$ as a function of distance r along the spin chain on a log-log scale for (a) $J_k/t = 0$, (b) $J_k/t = 1.5$, (c) $J_k/t = 2$ and (d) $J_k/t = 3$ at $J_h/t = 1$ and $L_x = L_y = L = \beta t$. The gray dashed line corresponds to $1/r$ decay and the insets plot the corresponding $S(k)$.

To confirm the above, we have computed the spin susceptibility $\chi(k) = \int_0^\beta d\tau S(k,\tau)$ with $S(k,\tau)$ given as

$$S(k,\tau) = \sum_r e^{-ik\cdot r} \langle \hat{S}^z(r,\tau) \hat{S}^z(r=0,\tau=0) \rangle. \quad (3)$$

Lorentz invariance at low energies implies that the time displaced correlation function scales as $1/\sqrt{r^2 + (v_s\tau)^2}$ with v_s the spin velocity. Setting $\beta t = L$, we hence expect $\chi(k = \pi)$ to diverge as L. Figure 4(a) plots $\chi(k = \pi)$ at $\beta t = L = 4n + 2$. Similar data at $L = 4n + 4$ can be found in Fig. S7 of Ref. [27]. For both cases we see two phases, one in which $\chi(k = \pi)$ scales as L and one in which it scales to a L-independent constant. In Fig. 4(b) we plot $(1/L)(\partial F/\partial J_k) = (2/3L)\sum_{l=1}^L \langle \hat{\boldsymbol{c}}_l^\dagger \boldsymbol{\sigma} \hat{\boldsymbol{c}}_l \cdot \hat{\boldsymbol{S}}_l \rangle$ so as to inquire the nature of the transition. The data favor a smooth curve, and hence a continuous quantum phase transition.

We now consider the dynamical spin structure factor, that relates to the imaginary-time correlation functions through $S(k,\tau) = (1/\pi)\int d\omega [e^{-\tau\omega}/(1 - e^{-\beta\omega})]\chi''(k,\omega)$. To extract $S(k,\omega) = [\chi''(k,\omega)/(1 - e^{-\beta\omega})]$, we use the stochastic analytical continuation algorithm [38]. The excitation spectrum of the isolated spin-1/2 Heisenberg chain is well understood and consists of a two-spinon continuum bounded by $(\pi/2)J_h \sin(k) \le \omega(k) \le \pi J_h \sin(k/2)$. Figure 5 plots the dynamical spin spectral function for different values of J_k/t. Remarkably, the spin dynamics of the Heisenberg chain remains unaffected by conduction electron for $J_k/t \lesssim 2$.

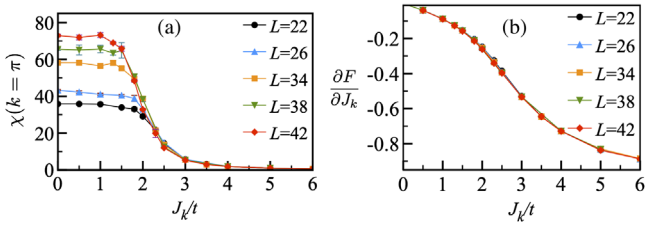

FIG. 4. (a) $\chi(k = \pi)$ as a function of J_k/t for $J_h/t = 1$ and $\beta t = L$. (b) Plots $\partial F/\partial J_k$ as a function of J_k/t.

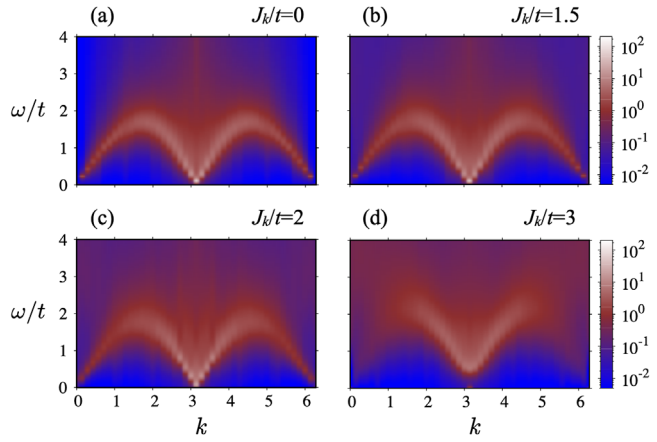

FIG. 5. $S(k,\omega)$ along spin chain as a function of energy (ω/t) and momentum (k) for $L=\beta t=44$ at $J_h/t=1$ and (a) $J_k/t=0$, (b) $J_k/t=1.5$, (c) $J_k/t=2$, and (d) $J_k/t=3$.

In the screened phase at $J_k/t>2$ spinons bind and low-energy spectral weight is depleted.

In Kondo lattices, a Kondo-breakdown transition implies an abrupt change of the Luttinger volume. In our setup such a notion cannot be applied since the localized spin-1/2 moments are subextensive. Nevertheless, we can consider the spectral function of the conduction electrons that directly couple to the localized spin-1/2 moments and investigate how it evolves across the transition. Let $A_n(k,\omega)=-(1/\pi)\mathrm{Im}G_n^{\mathrm{ret}}(k,\omega)$ with $G_n^{\mathrm{ret}}(k,\omega)=-i\int_0^\infty dt e^{i\omega t}\sum_\sigma\langle\{\hat{c}_{k,n,\sigma}(0),\hat{c}_{k,n,\sigma}^\dagger(t)\}\rangle$. In the considered Landau gauge, translation symmetry is present along the x direction and $\hat{c}_{k,n,\sigma}=(1/\sqrt{L})\sum_{m=1}^{L}e^{ikm}\hat{c}_{i=(m,n),\sigma}$ is the partial Fourier transform. Figure 6 plots $A_0(k,\omega)$ corresponding to the conduction electrons that couple to the Heisenberg chain. At $J_k=0$ the spectral function shows a dominant $\epsilon(k)=2t\cos(ka)$ dispersion. In the Kondo-breakdown phase and even at relatively large values of $J_k/t=1.5$ we observe no signs of hybridization with the spins. In contrast in the Kondo-screened phase $J_k/t\gtrsim 2$, a clear signature of hybridization is apparent.

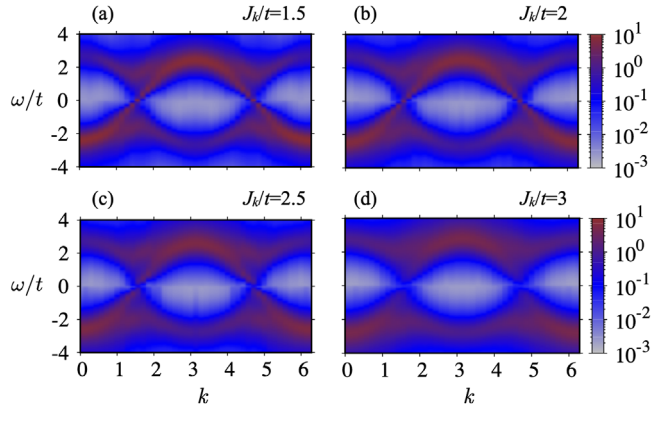

FIG. 6. $A_0(k,\omega)$ as a function of energy (ω/t) and momentum (k) for $L=\beta t=44$ at $J_h/t=1$ and (a) $J_k/t=1.5$, (b) $J_k/t=2$, (c) $J_k/t=2.5$, and (d) $J_k/t=3$.

STM experiments of magnetic adatoms on metallic surfaces, separated by an insulating buffer layer shown in Refs. [13,14], measure tunneling between tip and substrate occurring through the localized orbitals. In our setup we can access this quantity by carrying out a Schrieffer-Wolff transformation of the localized electron creation operator in the realm of the Anderson model [20,39,40]. In particular, $A_l(\omega)=-\mathrm{Im}G_l^{\mathrm{ret}}(\omega)$ with $G_l^{\mathrm{ret}}(\omega)=-i\int_0^\infty dt e^{i\omega t}\sum_\sigma\langle\{\tilde{c}_{l,\sigma}(t),\tilde{c}_{l,\sigma}^\dagger(0)\}\rangle$ and $\tilde{c}_{l,\sigma}^\dagger=\hat{c}_{l,-\sigma}^\dagger\hat{S}_l^\sigma+\sigma\hat{c}_{l,\sigma}^\dagger\hat{S}_l^z$. Here, $\sigma=\pm$ runs over the two spin polarizations and $\hat{S}_l^\pm=\hat{S}_l^x\pm i\hat{S}_l^y$. To evaluate the zero-bias tunneling signal we estimate $A_l(\omega=0)\simeq(1/\pi)\beta G_l(\tau=\beta/2)$. Figure 7 plots this quantity. Remarkably, in the Kondo-breakdown phase, we are not able to distinguish the signal from zero. This supports the notion that spins and conduction electrons decouple at low energies. As $J_k\to\infty$, the spin binds in a singlet with the conduction electron and the tunneling signal through the adatom drops. A more detailed numerical analysis [41,42] of the STM signal across the transition is certainly of great interest.

Conclusion.—We have shown that a one-dimensional spin chain coupled via a Kondo interaction to 2D Dirac fermions provides a realization of a continuous Kondo-breakdown transition. Weak coupling J_k is irrelevant and gapless propagating spinons exist, akin to an FL* phase. Beyond the transition, Kondo screening appears and gapless spinons bind. The Kondo-screened phase is adiabatically connected to the strong-coupling limit, where each spin binds with a conduction electron into a spin singlet. Larger systems will be needed to determine the critical exponents such as the anomalous dimension of the local moments. In addition, since the number of adatoms in experiments is tunable [14–16], it will be very useful to determine how many of them are needed to resolve Kondo breakdown in an interacting spin chain.

The choice of Dirac fermions which only possess Fermi points simplifies the problem and allows for an RG

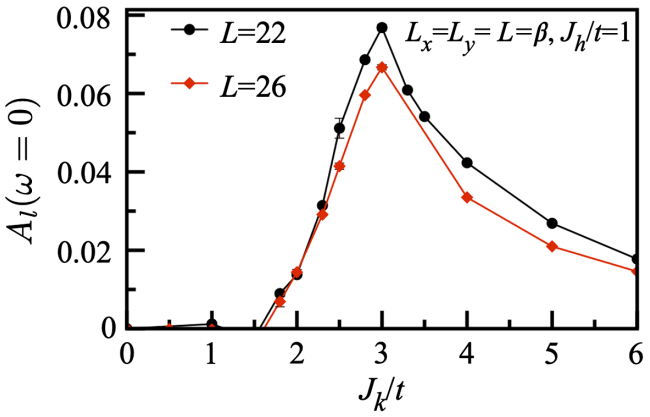

FIG. 7. Zero-bias tunneling through the magnetic adatom.

analysis. This is in contrast to the conventional Hertz-Millis-Moriya approach [43–45] where one integrates out the fermions to obtain an effective nonlocal action for local moments. Indeed, past work on Fermi surface coupled to a spin chain employed Hertz-Millis-Moriya approach, and concluded that the Kondo interaction is relevant (marginal) for an XXZ (Heisenberg) chain, thus destabilizing the Luttinger liquid for infinitesimal Kondo coupling [46]. In our problem, the irrelevancy of the Kondo interaction at the decoupled fixed point ($J_k = 0$) continues to hold even for a U(1) symmetric XXZ spin chain and we expect that the qualitative features of our phase diagram will remain unchanged. It will be desirable to study the problem of a Fermi surface coupled to an XXZ chain using QMC methods, which would also help bridge the gap with experiments in Refs. [13–19]. In addition, other scenarios for Kondo breakdown, such as the one discussed in Ref. [47], can also be studied using QMC.

In summary, we studied a problem of a spin chain coupled to Dirac fermions and established a Kondo-breakdown transition using a combination of techniques. Our results open the window to design and inform new experiments, along the lines of Refs. [14–16], where adatoms can be suitably arranged on metal-semimetal surfaces.

The authors thank M. Aronson, T.-C. Lu, J. McGreevy for useful conversations, and F. Mila for insightful collaborations on a related subject. The authors gratefully acknowledge the Gauss Centre for Supercomputing e.V. for providing computing time on the GCS Supercomputer SUPERMUC-NG at Leibniz Supercomputing Centre. The research has been supported by the Deutsche Forschungsgemeinschaft through Grant No. AS 120/14-1 (F. F. A), the Würzburg-Dresden Cluster of Excellence on Complexity and Topology in Quantum Matter—ct.qmat (EXC 2147, Project No. 390858490) (F. F. A. and M. V.), and SFB 1143 (Project No. 247310070) (M. V.). T. G. is supported by the National Science Foundation under Grant No. DMR-1752417, and as an Alfred P. Sloan Research Fellow. F. F. A. and T. G. thank the Bavaria California Technology Center for partial financial support.

*bimla.danu@physik.uni-wuerzburg.de
†matthias.vojta@tu-dresden.de
‡fakher.assaad@physik.uni-wuerzburg.de
§tagrover@ucsd.edu

[1] D. Withoff and E. Fradkin, Phys. Rev. Lett. **64**, 1835 (1990).
[2] L. Fritz and M. Vojta, Phys. Rev. B **70**, 214427 (2004).
[3] L. Fritz and M. Vojta, Rep. Prog. Phys. **76**, 032501 (2013).
[4] M. Vojta, J. Low Temp. Phys. **161**, 203 (2010).
[5] M. Yamanaka, M. Oshikawa, and I. Affleck, Phys. Rev. Lett. **79**, 1110 (1997).
[6] M. Oshikawa, Phys. Rev. Lett. **84**, 3370 (2000).
[7] T. Senthil, S. Sachdev, and M. Vojta, Phys. Rev. Lett. **90**, 216403 (2003).
[8] J. S. Hofmann, F. F. Assaad, and T. Grover, Phys. Rev. B **100**, 035118 (2019).
[9] P. Coleman, C. Pépin, Q. Si, and R. Ramazashvili, J. Phys. Condens. Matter **13**, R723 (2001).
[10] Q. Si, S. Rabello, K. Ingersent, and J. L. Smith, Nature (London) **413**, 804 (2001).
[11] S. Paschen, T. Lühmann, S. Wirth, P. Gegenwart, O. Trovarelli, C. Geibel, F. Steglich, P. Coleman, and Q. Si, Nature (London) **432**, 881 (2004).
[12] M. Klein, A. Nuber, F. Reinert, J. Kroha, O. Stockert, and H. v. Löhneysen, Phys. Rev. Lett. **101**, 266404 (2008).
[13] A. Spinelli, M. Gerrits, R. Toskovic, B. Bryant, M. Ternes, and A. F. Otte, Nat. Commun. **6**, 10046 (2015).
[14] R. Toskovic, R. van den Berg, A. Spinelli, I. S. Eliens, B. van den Toorn, B. Bryant, J. S. Caux, and A. F. Otte, Nat. Phys. **12**, 656 (2016).
[15] D. J. Choi, R. Robles, S. Yan, J. A. J. Burgess, S. Rolf-Pissarczyk, J. P. Gauyacq, N. Lorente, M. Ternes, and L. Sebastian, Nano Lett. **17**, 6203 (2017).
[16] M. Moro-Lagares, R. Korytr, M. Piantek, R. Robles, N. Lorente, J. I. Pascual, M. R. Ibarra, and D. Serrate, Nat. Commun. **10**, 2211 (2019).
[17] J. Bork, Y.-h. Zhang, L. Diekhner, L. Borda, P. Simon, J. Kroha, P. Wahl, and K. Kern, Nat. Phys. **7**, 901 (2011).
[18] L. Zhou, J. Wiebe, S. Lounis, E. Vedmedenko, F. Meier, S. Blgel, P. H. Dederichs, and R. Wiesendanger, Nat. Phys. **6**, 187 (2010).
[19] D. Serrate, P. Ferriani, Y. Yoshida, S.-W. Hla, M. Menzel, K. von Bergmann, S. Heinze, A. Kubetzka, and R. Wiesendanger, Nat. Nanotechnol. **5**, 350 (2010).
[20] B. Danu, F. F. Assaad, and F. Mila, Phys. Rev. Lett. **123**, 176601 (2019).
[21] L. Wu, W. Gannon, I. Zaliznyak, A. Tsvelik, M. Brockmann, J.-S. Caux, M. Kim, Y. Qiu, J. Copley, G. Ehlers *et al.*, Science **352**, 1206 (2016).
[22] W. J. Gannon, I. A. Zaliznyak, L. S. Wu, A. E. Feiguin, A. M. Tsvelik, F. Demmel, Y. Qiu, J. R. D. Copley, M. S. Kim, and M. C. Aronson, Nat. Commun. **10**, 1123 (2019).
[23] L. Classen, I. Zaliznyak, and A. M. Tsvelik, Phys. Rev. Lett. **120**, 156404 (2018).
[24] T. Giamarchi, *Quantum Physics in One Dimension* (Oxford University Press, New York, 2003).
[25] J. Cardy, *Scaling and Renormalization in Statistical Physics*, Cambridge Lecture Notes in Physics (Cambridge University Press, Cambridge, 1996).
[26] H. Tsunetsugu, M. Sigrist, and K. Ueda, Rev. Mod. Phys. **69**, 809 (1997).
[27] See Supplemental Material at http://link.aps.org/supplemental/10.1103/PhysRevLett.125.206602 for details of RG analysis, the large-N mean field calculation, and the QMC results, which include Ref. [28].
[28] J. A. Nelder and R. Mead, Comput. J. **7**, 308 (1965).
[29] Going beyond large-N, at $J_h = 0$, one obtains a Ruderman-Kittel-Kasuya-Yosida (RKKY) driven Heisenberg-interaction proportional to J_k^2 which decays as $1/r^4$, and whose ground state has the same universal properties as the nearest-neighbor model [30]. At small J_k, this RKKY interaction will dominate the Kondo scale $\sim e^{-W/J_k}$ where W is the bandwidth, and yields the same phase diagram as in Fig. 2.

[30] N. Laflorencie, I. Affleck, and M. Berciu, J. Stat. Mech. (2005) P12001.
[31] M. Bercx, F. Goth, J. S. Hofmann, and F. F. Assaad, SciPost Phys. **3**, 013 (2017).
[32] R. Blankenbecler, D. J. Scalapino, and R. L. Sugar, Phys. Rev. D **24**, 2278 (1981).
[33] S. R. White, D. J. Scalapino, R. L. Sugar, E. Y. Loh, J. E. Gubernatis, and R. T. Scalettar, Phys. Rev. B **40**, 506 (1989).
[34] F. F. Assaad and H. G. Evertz, in *Computational Many-Particle Physics*, Lecture Notes in Physics Vol. 739, edited by H. Fehske, R. Schneider, and A. Weiße (Springer, Berlin Heidelberg, 2008), pp. 277–356.
[35] F. F. Assaad, Phys. Rev. Lett. **83**, 796 (1999).
[36] S. Capponi and F. F. Assaad, Phys. Rev. B **63**, 155114 (2001).
[37] M. Raczkowski and F. F. Assaad, Phys. Rev. Research **2**, 013276 (2020).
[38] K. S. D. Beach, arXiv:cond-mat/0403055.
[39] M. Raczkowski and F. F. Assaad, Phys. Rev. Lett. **122**, 097203 (2019).
[40] T. A. Costi, Phys. Rev. Lett. **85**, 1504 (2000).
[41] D. J. Luitz, F. F. Assaad, T. Novotný, C. Karrasch, and V. Meden, Phys. Rev. Lett. **108**, 227001 (2012).
[42] C. Karrasch, V. Meden, and K. Schönhammer, Phys. Rev. B **82**, 125114 (2010).
[43] J. A. Hertz, Phys. Rev. B **14**, 1165 (1976).
[44] A. J. Millis, Phys. Rev. B **48**, 7183 (1993).
[45] T. Moriya, *Spin Fluctuations in Itinerant Electron Magnetism* (Springer Science & Business Media, New York, 2012), Vol. 56.
[46] A. M. Lobos, M. A. Cazalilla, and P. Chudzinski, Phys. Rev. B **86**, 035455 (2012).
[47] Y. Komijani and P. Coleman, Phys. Rev. Lett. **122**, 217001 (2019).